Randomized Optimal Design of Parallel Manipulators

Yunjiang Lou, *Student Member, IEEE*, Guanfeng Liu, and Zexiang Li, *Member, IEEE*

***Abstract*— This work intends to deal with the optimal kinematic synthesis problem of parallel manipulators under a unified framework. Observing that regular (e.g., hyper-rectangular) workspaces are desirable for most machines, we propose the concept of *effective regular workspace*, which reflects simultaneously requirements on the workspace shape and quality. The effectiveness of a workspace is characterized by the dexterity of the mechanism over every point in the workspace. Other performance indices, such as manipulability and stiffness, provide alternatives of dexterity characterization of workspace effectiveness. An optimal design problem, including constraints on actuated/passive joint limits and link interference, is then formulated to find the manipulator geometry that maximizes the effective regular workspace. This problem is a constrained nonlinear optimization problem without explicitly analytical expression. Traditional gradient based approaches may have difficulty in searching the global optimum. The controlled random search technique, as reported robust and reliable, is used to obtain an numerical solution. The design procedure is demonstrated through examples of a Delta robot and a Gough-Stewart platform.**

***Index Terms*— optimal design, parallel manipulators, effective regular workspace, controlled random search.**

I. Introduction

PARALLEL manipulators are widely accepted as ideal candidates for use in manufacturing industries for their potential superior properties over serial counterparts, such as low inertia, high stiffness, and high precision. However, relatively small workspace, complex input-output relationship, and abundance of singularities in their workspaces negate parts of above mentioned advantages. Choosing a set of geometric parameters so as to achieve desired/optimal performance is of vital significance in robotics research.

Among all kinematic measures, workspace is a basic yet most important index in design of a parallel manipulator. In regard to workspace requirements, there are two types of formulation of the design problem. One is to generate a manipulator whose workspace contains a prescribed workspace [1][2][3] [4][5]. Gosselin and Guillot [6] presented an algorithm for the workspace optimization of planar manipulators, where the objective is to obtain a workspace that is as close as possible to a prescribed one. The other possible formulation is to find the geometry of a parallel manipulator that maximizes workspace. A parallel manipulator designed only for maximum workspace may not however be a good design in practice. It is possible that the manipulator with maximum workspace has undesirable kinematic characteristics such as poor dexterity or manipulability. Stamper, Tsai, and Walsh [7] indicated this problem through an example of a 3 degree-of-freedom (DoF) translational parallel manipulator.

In order to avoid undesirable effects of workspace maximization, researchers introduced other performance indices into the optimal design problem. Gosselin and Angeles designed a planar [8] and a spherical [9] 3-DoF parallel manipulator by maximizing the workspace volume while taking into account the isotropy index. Pham and Chen [10] proposed to maximize the workspace of a parallel flexure mechanism subject to the constraints on a global measure and a uniformity measure of manipulability. In [7] Stamper *et al.* proposed to maximize the total volume of well-conditioned workspace, which is given as the integral of inverse condition number of the kinematic Jacobian matrix over the workspace. In addition to the workspace volume index, Stock and Miller [11] employed a linear combination of measures on manipulability and workspace in the objective function, where coefficients are weights assigned to the two indices. The optimal design problem then becomes a mixed multi-criteria optimization problem.

In this paper, we propose a unified formulation for optimal design of parallel manipulators. The design objective is to maximize *effective regular workspace*, defined to be the regular geometric object, e.g. a cube, a ball, or a cylinder in 3-dimensional case, every point of which not only is contained in the manipulator workspace, but also is effective for individual applications. In [12], Chablat *et al.* presented a similar design objective termed regular dextrous Cartesian workspace in performance comparison of two translational parallel machines, the Orthoglide and the UraneSX. The "dextrous" there imposes an interval constraint on all singular values of Jacobian in the regular workspace. It was proposed for optimal design of 3-DoF purely translational parallel mechanisms. In practice a regular-shaped workspace is desirable. It is well known that parallel manipulators often have irregular-shaped workspaces due to their complex kinematic structure. A design solely for maximal workspace may not have the maximal regular workspace. Furthermore, a design solely for maximal *regular* workspace may also lead to an undesirable result since there is no criterion guaranteeing the quality of workspace. It is

This research is supported in part by Hong Kong RGC grants No. HKUST 6301/03E, 616805, HKUST6187/01E and HKUST 6276/04E, and in part by NSFC grants No.50505009 and 50535010.

Yunjiang Lou is with the Department of Electronic and Computer Engineering (ECE), The Hong Kong University of Science and Technology (HKUST), Clear Water Bay, Kowloon, Hong Kong, China (email: louyj@ust.hk).

Guanfeng Liu was with the Dept. of ECE, HKUST, and is now with the Division of Control and Mechatronics Engineering (CoME), HIT Shenzhen Graduate School (HIT SZGS), China.

Zexiang Li is with the Dept. of ECE, HKUST, and the CoME Division of HIT SZGS (email: eezxli@ee.ust.hk).

possible that large zones of the workspace are ineffective and inapplicable for individual applications. In this paper, dexterity index is utilized to measure the effectiveness of workspace. Different indices can be adopted for different applications, such as stiffness, accuracy, and force/velocity transmission factors[13][14]. The optimal design problem is formulated to maximize the volume of regular-shaped workspace while subject to dexterity constraints.

The optimal design problem is a multimodal constrained nonlinear optimization problem with no explicit analytical expression. Gradient-based algorithms are not suitable for solving this problem since gradients and Hessians are not easily evaluated and they generally converge to local minima. Direct search methods seem to be good candidates. Usually people use exhaustive search to solve the problem [7][11][4]. Su *et al.* [15] and Arsenault and Boudreau [16] proposed genetic algorithm in solving optimal design problems. Recently, interval analysis based approaches have been applied to solve optimal design problems [12][17]. They can determine a design parameter space that satisfies all design constraints. Optimum is thus obtained by sampling the parameter space. However, the interval analysis based algorithms require explicitly analytic expressions of all constraints. They can not deal with constraints with no analytic expression. In our formulation, it is very difficult, even impossible to express all constraints in analytic forms. In this paper, the controlled random search (CRS) technique, which is a direct search method regardless of form of constraints and requires only evaluation of objective function and constraints, is applied.

Random search techniques were first proposed by Anderson [18] in 1953 and later by Brooks [19], Rastrigin [20], and Karnopp [21]. The random search techniques feature several advantages [21]. (1) *Ease of programming and realization*. Anyone can readily apply the technique in his individual application without advanced optimization knowledge. (2) *Robustness*. Practically, random search techniques are capable of handling discontinuous, non-differentiable objective functions with a nonconvex feasible region. (3) *Efficiency*. Although reports [22] showed that random search techniques converge quite slowly in the very close neighborhood of the optimum, they do converge efficiently to within 0.1% of the optimum. (4) *flexibility*. It is easy to modify the search procedure and combine heuristic knowledge and experience in the algorithm.

The major contributions of the paper are twofold. First, a unified design framework, including constraints on actuated/passive joint limits and link interference, is proposed. Second, a robust and reliable optimization approach, the CRS technique, is applied first time to solve optimal design problems. The paper is organized as follows. In section II, we formulate an optimization problem for design of parallel manipulators. In section III, a basic CRS algorithm and its real implementation are provided for solving the optimal design problem. In Section IV, a rotational Delta robot and a Gough-Stewart platform are used as examples to indicate the design procedure and technique. A conclusion is drawn in Section V.

II. Formulation of the optimal design problem

In this paper, we focus on normally actuated parallel manipulators where the number of actuators is equal to the number of DoFs of the manipulator. For an m-DoF normally actuated parallel manipulators, let $\theta \in \mathbb{R}^m$ and $\varphi \in \mathbb{R}^{n-m}$ respectively be sets of actuated and passive joint variables, and $X \in \mathbb{R}^m$ the Cartesian coordinate representing the position and orientation of the end-effector. Given an X, inverse kinematics maps can be derived as follows.

$$\theta_i = \theta_i(X, \alpha), \quad i = 1, \cdots, m \tag{1}$$

$$\varphi_i = \varphi_i(X, \alpha), \quad i = 1, \cdots, n-m \tag{2}$$

where α is the set of kinematic parameters, e.g., the link lengths, the position of base points of each subchain, the relative arrangement of each axis, and the size and shape of the end-effector, etc. In practice, we may only focus on a subset of those parameters, known as design parameters, while fixing remaining parameters according to some practical restrictions. Hereafter $\alpha \in \mathbb{R}^p$ denotes only the set of design parameters of interest, where p is the number of design parameters. The velocity relation can in general be written as

$$\dot{X} = J\dot{\theta}, \tag{3}$$

where $J = J(X, \theta, \alpha)$ is the kinematic Jacobian matrix, mapping joint rate $\dot{\theta}$ to Cartesian velocity $\dot{X}$.

A. The objective function

In manipulator design, a regular workspace (more specifically, a hyperrectangle) is usually provided as a design objective based on the types of manufacturing tasks and the working environment. This regular workspace is required to be contained in the workspace generated by the resultant manipulator such that it can conduct prescribed tasks. Maximization of the regular workspace among all possible designs is always desirable from the manufacturing perspectives.

Let $W = W_1 \times W_2$ be a regular workspace for a general parallel manipulator, where $W_1 \subset \mathbb{R}^3$ is the translational workspace and $W_2 \subset SO(3)$ the orientational workspace. A measure for W can be derived based on measures for W_1 and W_2. For example, let us assume that W_1 is a parallelepiped with l, w, h being lengths of three independent edges. The size of regular translational workspace is thus a function of those quantities. Let $\Phi_1 = \Phi_1(l, w, h)$ be a measure for the volume of W_1. The measure for the orientational workspace W_2 depends on types of application. For a machining application, the tilting capability plays a central role while the rotation about spindle axis is useless. For a dextrous manipulation case, the rotation about each axis is important. Let Φ_2 be a measure for the volume of W_2, a measure on the overall volume of W is given as

$$\Phi = \mu_1 \Phi_1 + \mu_2 \Phi_2, \tag{4}$$

where μ_i, $i = 1, 2$ are constants weighting contributions of W_1 and W_2, respectively. They are assigned according to different practical requirements.

Let us consider two special cases for (4). (i) When the

manipulator possesses no rotational motion, i.e., $\Phi_2 = 0$, or W_2 is fixed as a prescribed orientation capability, i.e., Φ_2 is constant, the objective function is then reduced to $\Phi = \Phi_1$. The objective of the problem is to maximize the translational regular workspace given that at each point in the translational regular workspace the manipulator at least possesses an orientational capability of W_2. Examples of this type include design of all kinds of translational parallel manipulators (e.g., the 3-UPU manipulator [23], the Delta robot [24], and the Orthoglide[13]) and k-DoF ($k > 3$) manipulators where a prescribed orientational capability is applied. (ii) When the manipulator undergoes purely rotation, i.e., $\Phi_1 = 0$, or W_1 is fixed as a prescribed translational regular workspace, i.e., Φ_1 is constant, the size function is reduced to $\Phi = \Phi_2$. Examples of this type include design of orientational parallel manipulators (e.g., the 3-DoF spherical manipulator) and k-DoF ($k > 3$) manipulators where a maximal orientation capability is desirable in a prescribed translational workspace. In this paper, we demonstrate the design technique using the first case for optimal design of two typical parallel manipulators.

It is well-known that given fixed ranges of actuators of a parallel manipulator, its workspace volume monotonically depends on its overall dimension i.e., the value α takes. By considering the constraints due to working environments, we normalize the manipulator dimension so as to find the best design among all normalized manipulators with the same topology. The result is expected to provide an insight and a basic guidance for practical realization.

$$\sum_{i=1}^{q} \alpha_i = \tau, \tag{5}$$

where τ is a given constant, usually 1, and $\alpha_i \geq 0,\ i = 1, \cdots, q$ are geometric parameters, and $q \leq p$. The equation (5) implies that $\alpha_i \in [0, \tau],\ i = 1, \cdots, q$.

B. The workspace constraints

A basic requirement for a regular workspace is that it should be contained in the workspace generated by the resultant manipulator. The workspace of a manipulator is determined by the manipulator's geometry and actuated/passive joint limits. As well known, a point X is reachable if there exists an inverse kinematic solution θ in the actuator range. A set W is reachable means every $X \in W$ is reachable. Specifically, it is equivalent to impose the following constraints to every point $X \in W$,

$$\rho_i^{min} \leq \rho_i(X, \alpha) \leq \rho_i^{max}, \quad i = 1, \cdots, m; \tag{6}$$

where ρ_i^{min} and ρ_i^{max} are respectively the lower and upper bound for i-th actuator due to actuator limits. The expression (6) provides a necessary condition for a point to be in the workspace. However, there may often exist limits for passive joints. Given passive joint limits $[\varphi_k^{min}, \varphi_k^{max}]$, a point X is in the workspace also means

$$\varphi_k^{min} \leq \varphi_k(X, \alpha) \leq \varphi_k^{max}, \quad k = 1, \cdots, n - m. \tag{7}$$

Because of the complex architecture of a parallel manipulator, mechanical interference may occur among its links in motion. It surely reduces workspace. Assume that the manipulator is composed of t links. For simplicity, each link is approximated by the minimal cylinder enclosing the link. Let the radius of the cylinder be R_i and denote by $\mathbf{L}_i$ the line segment passing the i-th cylinder axis, $i = 1, \cdots, t$. Clearly there is no mechanical interference if the distance between any pair of line segments is larger than the sum of corresponding radii. Fig. 1 depicts the distance between two cylinder-modelled links. The following inequalities ensure that no link interference will occur for a point X.

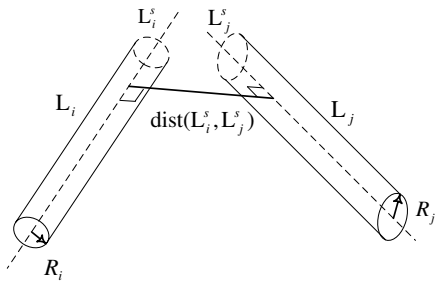

Fig. 1. The distance between two links

$$\mathrm{dist}(\mathbf{L}_i, \mathbf{L}_j) \geq R_i + R_j, \quad i, j = 1, \cdots, t;\ i \neq j, \tag{8}$$

where $\mathrm{dist}(\mathbf{L}_i, \mathbf{L}_j)$ is the function computing the distance between two line segments $\mathbf{L}_i$ and $\mathbf{L}_j$. Note $\mathbf{L}_i = \mathbf{L}_i(X, \alpha)$.

The set of points satisfying (6)-(8) constitute the workspace reachable by the resultant parallel manipulator. Therefore, any point $X \in W$ should satisfy (6)-(8).

C. The dexterity constraints

In order to guarantee the regular workspace to be effective, constraints on the dexterity index are introduced to characterize quality of the regular workspace. The dexterity index describes the ability of a mechanism to move and apply forces in arbitrary directions as easily as possible. A frequently-used measure for dexterity is the inverse condition number of the kinematic Jacobian matrix, which is defined as

$$\kappa(J) = \frac{\sigma_{min}(J)}{\sigma_{max}(J)},$$

where $\kappa(\cdot)$ denotes the inverse condition number function of matrices, and $\sigma_{min}(\cdot)$ and $\sigma_{max}(\cdot)$ its minimal and maximal singular value functions, respectively. Thus $\kappa \in [0, 1]$.

This performance measure has been applied in numerous designs since it characterizes various properties of a manipulator, such as singularity, local kinematic isotropy, relative control error, and uniformity of Cartesian stiffness. However, when a robot is capable of mixed motions of translation and orientation or when it is comprised of both rotary and prismatic actuators, elements of the kinematic Jacobian bear different physical units, i.e., the Jacobian is dimensionally in homogeneous. This measure inherently involves some sort of tradeoff between orientation and position. Any design based on it will probably produce misleading results [25]. Here we treat separately orientation and position dexterity. Let us rewrite the

differential kinematics (3) by

$$\begin{bmatrix} \dot{Z} \\ \dot{\Psi} \end{bmatrix} = \begin{bmatrix} J_z \\ J_\Psi \end{bmatrix} \dot{\theta},$$

where $\dot{Z}$ and $\dot{\Psi}$ are linear velocity and angular velocity, respectively. Thus, $\kappa(J_z)$ and $\kappa(J_\Psi)$ respectively give measures for position and orientation dexterity. To guarantee position and orientation dexterity, they are applied in design by imposing the following constraints

$$\kappa(J_z) \geq \gamma_1, \tag{9}$$
$$\kappa(J_\Psi) \geq \gamma_2, \tag{10}$$

where γ_1 and γ_2 are two thresholds for position and orientation dexterity, which are constants assigned according to practical design requirements.

Combining constraints (4)-(10), the optimal design problem for maximization of effective regular workspace is formulated as following.

Problem 1: Optimal mechanism design
Find a set of optimal design parameters α such that

$$\max_{\alpha} \quad \Phi(\alpha) \tag{11}$$
$$\text{subject to} \quad \kappa(J_z(X,\theta,\alpha)) \geq \gamma_1, \tag{12}$$
$$\kappa(J_\Psi(X,\theta,\alpha)) \geq \gamma_2, \tag{13}$$
$$\rho_i^{min} \leq \rho_i(X,\alpha) \leq \rho_i^{max}, \tag{14}$$
$$\varphi_j^{min} \leq \varphi_j(X,\alpha) \leq \varphi_j^{max}, \tag{15}$$
$$\text{dist}(\mathbf{L}_k, \mathbf{L}_l) \geq R_k + R_l, \tag{16}$$
$$\sum_{j=1}^{q} \alpha_j = \tau. \tag{17}$$

where $\forall X \in W$, $i = 1, \cdots, m$; $j = 1, \cdots, n-m$; $k, l = 1, \cdots, t; k \neq l$. ■

III. The CRS algorithm and its implementation

Clearly the optimal design problem 1 is a constrained nonlinear optimization problem. The objective function (11), the dexterity constraint (12), and the link interference constraint (16) have no explicitly analytical expressions with respect to the set of design parameters α. Gradients and Hessians are thus not readily computed. Furthermore, the objective function in the optimal design problem 1 is generally multimodal, i.e., there may exist many local minima in the feasible region. Those gradient based optimization algorithms, e.g., the sequential quadratic programming (SQP) methods, are known to converge to local minima. Here, we resort to a direct search method, the random search technique, which was widely studied as a global optimization technique [26]. The algorithms are robust, i.e., they normally work regardless of irregularities of the objective function and feasible region.

A. The Controlled Random Search Technique

In 1978, Goulcher and Long [27] proposed a controlled random search (CRS) method to solve constrained nonlinear optimization problems. Later this method was improved and applied in many chemical plants [28]. The basic philosophy of the method is to select new points by random selection from normal probability distributions centered at the best previous value

$$\alpha^{(j)} = \alpha^{(j-1)*} + \sigma\xi, \ j = 1, 2, \cdots. \tag{18}$$

The equation (18) describes how the new points in j-th iteration, $\alpha^{(j)}$, are generated in the neighborhood of the previous best point $\alpha^{(j-1)*}$, where ξ is a vector of random variables ξ_i that are subject to normal probability distribution with zero mean and unity standard deviation as follows.

$$\xi_i \sim N(0,1), \quad i = 1, \cdots, p.$$

$\sigma = \text{diag}(\sigma_1, \cdots, \sigma_p)$ is applied to adaptively modify the standard deviation of the normal probability distribution for every random variable in each iteration. It is actually the standard deviation for the vector of random variables $\sigma\xi$. Therefore, "control" comes by adjustment of the standard deviation of the distribution, which explains the name of the method. Compared with standard optimization techniques, the random variable ξ can be regarded as a search direction, while the standard deviation σ serves as a kind of "step-length", which is adjusted automatically during the search in two situations.

(a) Each time a successful trial has been made. In this case, standard deviations are set according to $\sigma_i = K_1\Delta\alpha_i$, $i = 1, \cdots, p$, where $\Delta\alpha_i$ is a positive quantity describing the distance between the variable's current value α_i and the nearest bound of the variable. $K_1 < 1$ is a compression factor to reduce search interval and maintain searches in the neighborhood of the best previous point.

(b) After a specified number, typically 100, of consecutive failure. Failure means that no improvement is made with respect to the objective function. When this occurs, for instance, as the optimum is approached, the standard deviations are reduced by

$$(\sigma_i)_{new} = K_2(\sigma_i)_{old}, \quad i = 1, \cdots, p;$$

where $K_2 < 1$ is a positive number.

The basic algorithm of the CRS technique is described as follows.

Algorithm *1:* The basic CRS algorithm

1) Given search intervals, $\alpha_i \in [\underline{\alpha_i}, \overline{\alpha_i}]$, set parameters K_1, K_2, ϵ, and max_feval denoting the maximum allowable number of function evaluation;
2) Generate a feasible initial point $\alpha^{(0)*}$ by uniformly random sampling in the given intervals, and compute the corresponding $\Phi^{(0)*}$ and $\sigma_i^{(0)} = K_1\Delta\alpha_i^{(0)}$, $i = 1, \cdots, p$. Set $j = 1$;
3) Set $k = 1$.
4) If $k > max\_feval$, set $\sigma_{new}^{(j-1)} = K_2\sigma_{old}^{(j-1)}$ and go to 3); otherwise, generate a new search point by

$$^k\alpha^{(j)} = \alpha^{(j-1)*} + \sigma^{(j-1)}\xi,$$

verify all constraints at $^k\alpha^{(j)}$. Set $\Phi(^k\alpha^{(j)}) = -M$ if not all constraints are satisfied, where M is a number large enough; otherwise, evaluate $\Phi(^k\alpha^{(j)})$.

5) If $\Phi({}^k\alpha^{(j)}) \leq \Phi^{(j-1)*}$, set $k = k+1$, go to 4); otherwise, set $\Phi^{(j)*} = \Phi({}^k\alpha^{(j)})$ and $\alpha^{(j)*} = {}^k\alpha^{(j)}$.
6) Check the stopping criterion

$$\frac{|\alpha_i^{(j)*} - \alpha_i^{(j-1)*}|}{R_i} \leq \epsilon, \quad i = 1, \cdots, p;$$

where $R_i = \overline{\alpha_i} - \underline{\alpha_i}$. If it is satisfied, stop the procedure; otherwise, set $j = j+1$ and go to 3).

Solis and Wets [29] proved global convergence for their conceptual algorithm. The CRS technique is a realization of the conceptual algorithm. Their proof needs only minimal technical assumptions, measurability of the objective function and the feasible set, that are always satisfied in practice. Readers are referred to [29] for detailed description.

B. The Real Implementation

The basic CRS algorithm provides a unified framework to solve optimization problems. The basic procedure is first to generate a point by the *normal* distribution around the previous best point, then to verify all constraints at this point, if all constraints are satisfied, evaluate the objective and compare it with the previous best objective. If there is no improvement or not all constraints are satisfied, generate a new point and repeat verification of constraints and evaluation of objective; otherwise, replace the previous best point/objective by the current point/objective and continue execution of generation, verification, evaluation, and comparison iteratively.

In implementation of the algorithm, users only need to specify the evaluation of objective functions and constraints in step 4) for individual problems. For the optimal design problem 1, it involves searching the maximal size of effective regular workspace at a generated value of α. Although the maximal size of effective regular workspace depends uniquely upon the design parameters, the search of the maximal size really involves finding the location of maximal effective regular workspace. Take a *cubic* effective workspace for instance, a usual scheme for searching of its maximal size is that (a) first choose a point in Cartesian workspace that satisfies all constraints as the center of the cubic workspace. If there is no such point, the maximal size of the cubic effective workspace is zero. And (b) take an adequately large side length and decrease it gradually until all constraints are fulfilled. This obtained value is therefore the largest side length of the cubic effective workspace corresponding to the center chosen in (a). By varying cube centers, different largest side lengths are obtained correspondingly. The maximal value of all those largest side lengths gives the maximal size for the cubic effective workspace corresponding to the generated value of α. If this maximal size is larger than the previous best, it and its current value of α will be stored to substitute the previous best. Otherwise, it will be discarded. Then, a new value of α will be generated by (18), and an execution of step (a) and (b) will give another largest side length corresponding to the new value of α. This search scheme involves execution of step (a) and (b) iteratively.

Another scheme is much simpler in philosophy. It regards the location of the effective regular workspace as part of design parameters, which are generated by (18) along with all other design parameters. When a value of the new set of design parameters α is generated, the corresponding maximal size can be searched by step (b). The search for the center of the maximal effective workspace and other optimal design parameters are conducted simultaneously. There is no difference in result for those two schemes. In the implementation the latter one is employed and the bisection technique is applied in search of the maximal size (step (b)).

Generally the randomly generated values of α do not satisfy the normalization equality (17). A simple treatment is used to deal with the problem. Assume $\alpha = [\alpha_1, \cdots, \alpha_q, \alpha_{q+1}, \cdots, \alpha_p]$, where the first q variables are geometric parameters appearing in the equality constraint (17) with $\alpha_i \in [0, t_i], i = 1, \cdots, q$. Without loss of generality, we take $\alpha_2, \cdots, \alpha_q$ as independent parameters, $\alpha_1 = \tau - \sum_{i=2}^{q} \alpha_i$, and $\tau \geq t_i$, $i = 1, \cdots, q$. The number of independent design parameters is reduced to $p-1$. Let us denote the set of independent parameters by $\tilde{\alpha} := [\tilde{\alpha}_1, \cdots, \tilde{\alpha}_{p-1}] = [\alpha_2, \cdots, \alpha_p]$. Values of $\tilde{\alpha}$ are generated uniformly (when initialization) or by (18) (otherwise). In the implementation, the following treatment is applied to deal with the randomly generated new points $\tilde{\alpha}$. $\alpha_2 = \tilde{\alpha}_1$, and for $i = 2, \cdots, q-1$,

$$\alpha_{i+1} = \begin{cases} \tilde{\alpha}_i, & \text{if } \tau - \sum_{k=1}^{i-1} \alpha_k \geq t_i \\ (\tau - \sum_{k=1}^{i-1} \alpha_k)\tilde{\alpha}_i / t_i, & \text{if } \tau - \sum_{k=1}^{i-1} \alpha_k < t_i \end{cases}$$

$\alpha_1 = \tau - \sum_{i=2}^{q} \alpha_i$, and $\alpha_{k+1} = \tilde{\alpha}_k$, $k = q, \cdots, p-1$. It is guaranteed that the normalization equality and interval constraints are satisfied. $\alpha = [\alpha_1, \cdots, \alpha_p]$ is then applied in evaluation of the objective and constraints. The α in Algorithm 1 should be considered as the set of independent parameters $\tilde{\alpha}$. The computed α in the treatment is used only to evaluate the objective and constraints.

In problem 1, the constraints (12)-(16) should be satisfied at every point of the regular workspace. In numerical computation, however, it is impossible to verify the constraints at all points. As people usually do, we discretize the regular workspace and only verify the constraints at the discretized nodes. This may lead to that some constraints are not satisfied at some points for a searched result. The effect can be reduced or eliminated by a finer discretization and/or assigning more stringent bounds in (12)-(16).

IV. Simulations and Results

In this section, a rotational Delta robot and a Gough-Stewart platform are employed as examples to demonstrate the design procedure.

A. Optimal design of a rotational Delta robot

The rotational Delta robot, as shown in Fig. 2, is a spatial parallel manipulator undergoing purely translational motion. Here, "rotational" means that the actuated joints on the base are rotary, which distinguishes the mechanism from its linear actuated counterpart. This architecture was invented by Clavel [24] and is well-known due to its very high speed. The mechanism consists of a base, a moving platform, and three

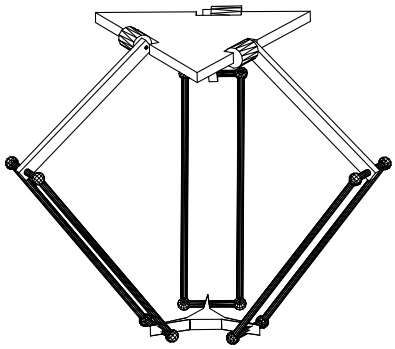

Fig. 2. Architecture of the rotational Delta robot

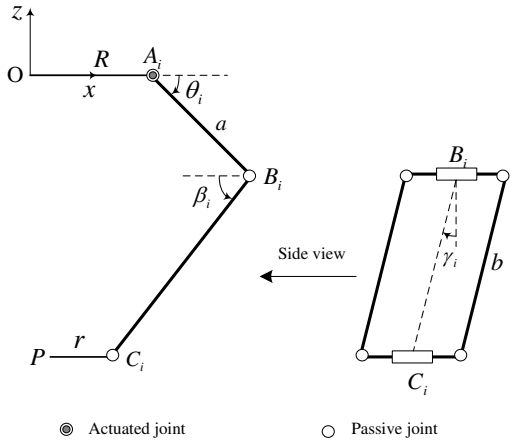

Fig. 3. The i-th subchain of the rotational Delta robot

identical subchains. All subchains have a common $\underline{\text{R}}\text{R}P_a\text{R}$ topology from base to the moving platform, where R denotes a *revolute* joint, P_a a *parallelogram*, and the underscored "R" an actuated revolute joint. Three actuated joints on the base are arranged symmetrically at the three vertices of an equilateral triangle, So are the three passive joints on the moving platform. The kinematic parameters are depicted in Fig. 3, where a denotes the length of arms A_iB_i, b the length of the parallelogram, and $R = \|OA_i\|$, $r = \|PC_i\|$, $i = 1, \cdots, 3$, with O and P being centers of the base and the moving platform, respectively.

Let us attach an inertia frame to the base center O such that the base is in the xy-plane and OA_1 points along the $+x$-axis. The $+z$-axis is arranged to point up and to be perpendicular to the base plane. From the geometry of the mechanism, a loop-closure constraint can be derived for each subchain as follows.

$$\overrightarrow{OP} = \overrightarrow{OA_i} + \overrightarrow{A_iB_i} + \overrightarrow{B_iC_i} + \overrightarrow{C_iP}, \tag{19}$$

for $i = 1, \cdots, 3$. Note that the vector equation (19) is composed of three scalar equations with three kinematic variables θ_i, β_i, and γ_i. Given the coordinate of the reference point P, $X = (x, y, z)^T$, we can solve inverse kinematics for θ_i, β_i, and γ_i from (19). By eliminating passive joint variables from (19), we derive loop-closure equations relating the actuated joint variable $\theta = (\theta_1, \theta_2, \theta_3)^T$ to X.

$$(x - (d + a\cos\theta_i)\cos\varphi_i)^2 + (y - (d + a\cos\theta_i)\sin\varphi_i)^2 + (z + a\sin\theta_i)^2 - b^2 = 0, \tag{20}$$

for $i = 1, \cdots, 3$, where $d = R - r$ and φ_i denotes the angle made by the i-th subchain and the $+x$-axis. In our symmetric arrangement, $\varphi_i = (i-1)\frac{2\pi}{3}$ for $i = 1, \cdots, 3$.

Differentiating the loop constraints (20) with respect to time t we obtain differential kinematics between the actuated joint rates and Cartesian velocities, $J_x\dot{X} = J_\theta\dot{\theta}$, where

$$J_x = \begin{bmatrix} v_1^T \\ v_2^T \\ v_3^T \end{bmatrix}, \tag{21}$$

with $v_i = [x - (d + a\cos\theta_i)\cos\varphi_i,\ y - (d + a\cos\theta_i)\sin\varphi_i,\ z + a\sin\theta_i]^T$, $i = 1, \cdots, 3$, and

$$J_\theta = -\text{diag}\{h_1, h_2, h_3\}, \tag{22}$$

with $h_i = (x\cos\varphi_i + y\sin\varphi_i - d)a\sin\theta_i + za\cos\theta_i$ for $i = 1, \cdots, 3$. Therefore, $J = J_x^{-1}J_\theta$.

In the design a cubic shape is chosen for the regular workspace W. Denoting by $2l$ the side length of the cubic workspace, we take the objective $\Phi = l$ to represent the workspace volume. The center of the resultant maximal effective regular workspace is undetermined and its coordinates are regarded as design parameters. Since the manipulator is symmetric with respect to the z-axis, the center should be in the z-axis. In other words, it has the form of $(0, 0, z_c)$. According to above analysis, a set of design parameters is thus determined, $\alpha = [a\ b\ d\ z_c]^T$. The manipulator size is normalized by subchain normalization $a + b + d = 1$. In this example, mechanical interference constraints (16) and manufacturing constraints are implicitly included by imposing the following constraints on the actuated and passive joints as in [30].

1) $-40^\text{o} \le \gamma_i \le 40^\text{o}$ due to constructional constraints on the parallelogram's articulations;
2) $45^\text{o} \le \theta_i + \beta_i \le 180^\text{o}$ is imposed in order to avoid interference between the arms and the parallelogram rods when the angle is acute and to avoid ambiguities in computation;
3) $-30^\text{o} \le \theta_i \le 100^\text{o}$ is chosen.

If for some applications the lower bound of dexterity is given as 0.4, by combining all other requirements together, the optimal design problem is formulated as follows.

Problem 2: Optimal design of a rotational Delta robot
Find a set of optimal design parameters α such that

$$\begin{aligned} \max_{\alpha} \quad & l \\ \text{subject to} \quad & \kappa(J(X, \theta, \alpha)) \ge 0.4; \\ & -30^\text{o} \le \theta_i(X, \alpha) \le 100^\text{o}; \\ & 45^\text{o} \le \theta_i + \beta_i \le 180^\text{o}; \\ & -40^\text{o} \le \gamma_i \le 40^\text{o},\ i = 1, \cdots, 3; \\ & a + b + d = 1; \\ & a,\ b,\ d \in [0, 1], \quad z_c \in [-1, 0]; \end{aligned}$$

	a	b	d	z_c	$\Phi^* = l^*$
$\gamma = 0.5$	0.5322	0.4300	0.0377	-0.6523	0.1136
$\gamma = 0.4$	0.5837	0.4064	0.0099	-0.6889	0.1296
$\gamma = 0.3$	0.6137	0.3855	0.0008	-0.7093	0.1434
$\gamma = 0.2$	0.6162	0.3709	0.0129	-0.7109	0.1542

TABLE I

OPTIMAL RESULTS FOR THE DELTA ROBOT

where $\forall X \in W$. ■

By applying the CRS algorithm, the optimal values of design parameters and the corresponding center and side length of the maximal effective cubic workspace are obtained for $\gamma = 0.2, 0.3, 0.4, 0.5$ and given in Table I. Fig. 4 shows a scaled 3D model of the resulting optimal mechanism for $\gamma = 0.4$. We note that d tends to zero for any value of γ, which implies that an identical size of the base and the moving platform is desirable for maximization of the effective regular workspace. We next verify workspace containment and inverse condition number constraints of the resulting optimal mechanism for the case of $\gamma = 0.4$.

By considering the joint limits, the workspace generated by the Delta robot is the intersection of a right hexagonal prism with infinite height and three identical revolution volumes with different axes, as shown in [24]. Fig. 5-(a), 6-(a), and 7-(a) show workspace cross sections generated by the resulting Delta robot at $z = z_c - l^*$, $z = z_c$, and $z = z_c + l^*$, respectively. The shaded squares in the figures correspond to cross sections of the maximal effective cubic workspace. In the Fig. 5-(a) and 6-(a), the maximal effective regular workspace cross sections are perfectly contained in the resulting workspace, while in the Fig. 7-(a) the cross section of the maximal effective regular workspace touches the workspace boundary of the resulting workspace, where the workspace constraints take effect.

Fig. 5-(b), 6-(b), and 7-(b) show distribution of inverse condition number at cross sections, respectively in the planes $z = z_c - l^*$, $z = z_c$, and $z = z_c + l^*$ of the maximal effective cubic workspace. In the former two cross sections, all inverse condition numbers are larger than the prescribed threshold, 0.4. The minimal κ in the cube is 0.3997, which occurs in the cross section $z = z_c + l^*$. This minimal κ is less than, but very close to the threshold. As shown in Fig. 7-(b), the minimal κ is NOT at the boundary of the maximal effective regular workspace. The condition number constraint (12) is violated. This error is introduced due to discretization of the regular workspace. In this example, the constraints were verified at only 9 points, the 8 vertices and the center of a cube. However, the introduced error is rather small and acceptable for an engineering design.

B. Optimal design of a general Gough-Stewart platform

A Gough-Stewart platform, as shown in Fig. 8, is composed of a fixed base, a moving platform, and six identical SPS legs. Here S denotes a **s**pherical joint while P is a **p**rismatic joint, and the base and the moving platform are assumed to be semi-hexagonal as conventional design of the manipulator. The moving platform is controlled by driving the P-joints to

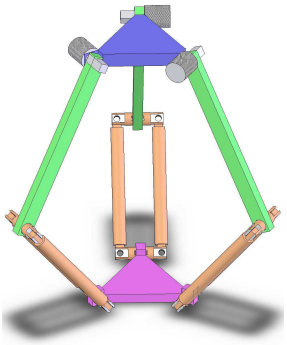

Fig. 4. A CAD model of the resulting Delta robot

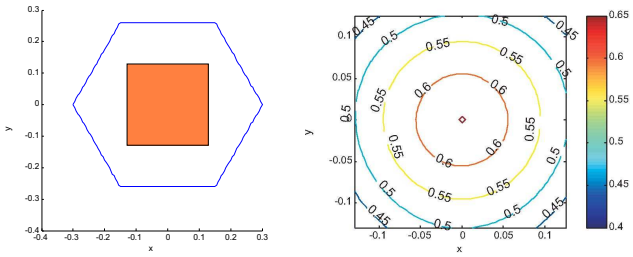

(a) (b)

Fig. 5. (a) Workspace cross section at $z = z_c - l^*$; (b) contour plot of the inverse condition number of J at $z = z_c - l^*$.

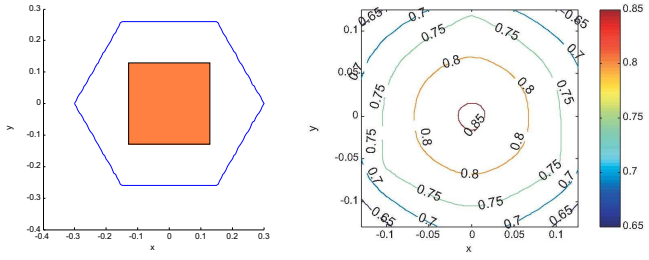

(a) (b)

Fig. 6. (a) Workspace cross section at $z = z_c$; (b) contour plot of the inverse condition number of J at $z = z_c$.

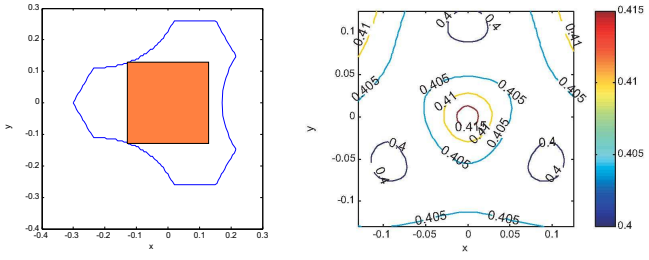

(a) (b)

Fig. 7. (a) Workspace cross section at $z = z_c + l^*$; (b) contour plot of the inverse condition number of J at $z = z_c + l^*$.

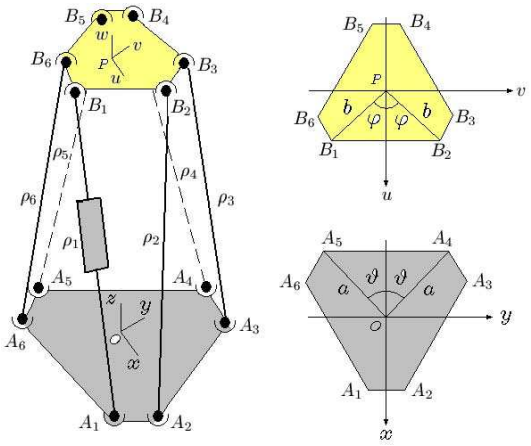

Fig. 8. A schematic for the Gough-Stewart platform

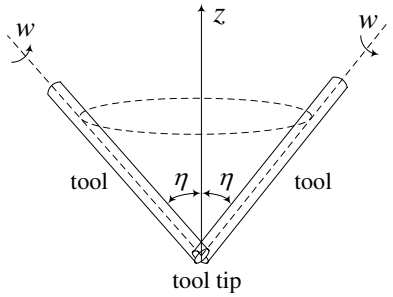

Fig. 9. Tilting angle η for a machine tool

extend/retract legs. The leg geometry is determined by the minimum leg length, which is measured when all actuators are zero actuated, and the stroke. Since only a few set of possible strokes are available for commercial linear actuators, we may choose it beforehand and modify other design parameters to adapt it. We therefore normalize the stroke by unity. From Fig. 8, the geometry of the manipulator is defined by five parameters, namely,

- a: the radius of the circle on the base where the S joint A_i lie;
- b: the radius of the circle on the moving platform where the S joint B_i lie;
- ϑ: half the angle between two far S joints on the base;
- φ: half the angle between two far S joints on the moving platform;
- ρ_0: the leg length when the manipulator is at its home position, where all actuators are at their half stroke.

An inertia frame O-xyz is set up at the base center with z-axis pointing vertically upward. A body frame P-uvw is similarly attached to the center of the moving platform with the w-axis normal to the platform, pointing outward. The frames are set up such that the x-axis passes perpendicularly both midpoints of A_1A_2 and A_4A_5, and u-axis passes both midpoints of B_1B_2 and B_4B_5 perpendicularly. At the home position the body frame is assumed to have the same orientation as the inertia frame.

The configuration of the moving platform can be described by both the position of the reference point $P = (x, y, z)$ and the orientation of the moving platform (β, ϕ, ψ), which are the ZYX Euler angles (yaw, pitch, and roll angles). Let the inverse kinematics map for the actuated joints be $\rho_i = \rho_i(X, \alpha)$, $i = 1, \cdots, 6$, and the differential kinematics map be

$$\begin{bmatrix} \dot{Z} \\ \dot{\Psi} \end{bmatrix} = \begin{bmatrix} J_z(X, \rho, \alpha) \\ J_\Psi(X, \rho, \alpha) \end{bmatrix} \dot{\rho}, \tag{23}$$

where $\dot{\rho} = [\dot{\rho}_1, \cdots, \dot{\rho}_6]^T$, $\dot{Z} = [\dot{x}\ \dot{y}\ \dot{z}]^T$, $\dot{\Psi} = [\dot{\psi}\ \dot{\phi}\ \dot{\beta}]^T$, $X = [x, y, z, \psi, \phi, \beta]^T$, and $\rho = [\rho_1, \cdots, \rho_6]^T$. Since the Gough-Stewart platform is capable of both translational and rotational motion, we separately treat position and orientation dexterity, as discussed in section II-C.

The effective regular workspace of the Gough-Stewart platform is composed of two portions, the translational one W_1 and the orientational one W_2. Let's consider the Gough-Stewart platform for machine tool applications. Suppose a spindle is attached to the reference point P and the spindle axis coincides with the w-axis. A practical workspace requirement is that the spindle (so the tool) be able to access a regular translational workspace with good tilting capability. The tilting capability of a machine tool is usually characterized by the tilting angle η, which is the maximum angle made by the spindle axis (w-axis) and z-axis that the machine is able to reach at every point in the regular workspace, as illustrated in Fig. 9. It is thus desirable to maximize the regular translational workspace constrained by a fixed threshold η_0 for tilting angle.

- *The objective*: A cube with side length $2l$ in $\mathbb{R}^3$ is designated as the translational workspace W_1. The objective function is chosen as $\Phi = l$, which is constrained by the tilting capability $\eta \geq \eta_0$ with $\eta_0 = 30^o$ in the simulation. The center of the maximal cubic workspace is taken as $[0, 0, z_c, 0, 0, 0]^T$ since the manipulator is architecturally symmetric about the z-axis. Thus the set of design parameters is determined, $\alpha = (a\ b\ \rho_0\ \vartheta\ \varphi\ z_c)$.
- *Constraints on dexterity*: The translation and orientation dexterity constraints are imposed with $\gamma_1 = 0.2$ and $\gamma_2 = 0.2$.
$$\kappa(J_z) \geq 0.2 \qquad \kappa(J_\Psi) \geq 0.2$$
- *constraints due to actuated joint limits*: As discussed above, the strokes are normalized by unity, i.e., the leg lengths ρ_i is constrained by
$$\rho_0 - 0.5 \leq \rho_i(X, \alpha) \leq \rho_0 + 0.5, \quad i = 1, \cdots, 6.$$
- *constraints due to passive joint limits:* Assume the ball joint range is $[0, \mathcal{B}]$, the constraints due to ball joint limits are given as follows.
$$0 \leq \text{Angle}(\mathbf{L}_j^w, \mathbf{L}_{j0}^w) \leq \mathcal{B};$$
$$0 \leq \text{Angle}(\mathbf{L}_j^b, \mathbf{L}_{j0}^b) \leq \mathcal{B};$$
where $\mathbf{L}_j^w$ and $\mathbf{L}_{j0}^w$ are line segments representing the pose of leg j at current configuration and the home configuration, respectively. The superscripts w and b are used to indicate in which frame the line segment is expressed: w for the world frame O-xyz and b for the

body frame P-uvw. When there is no confusion, we eliminate the superscript w for elements expressed in the world frame. $\text{Angle}(\mathbf{L}_j^w, \mathbf{L}_{j0}^w)$ and $\text{Angle}(\mathbf{L}_j^b, \mathbf{L}_{j0}^b)$ thus compute pivot angles of base ball joint and moving platform ball joint on the j-th leg, respectively. We take $\mathcal{B} = 55^\circ$ in the simulation.

- *Constraints due to leg interference*:

$$\text{dist}(\mathbf{L}_k, \mathbf{L}_l) \geq 2R, \quad k, l = 1, \cdots, 6; \ k < l,$$

where we assume an identical radius R for all legs. In the simulation R is two percents of the stroke, $R = 0.02$.

- *Constraints on manipulator size*: A constraint on the manipulator size is imposed as

$$a + \rho_0 + b = \lambda,$$

where λ is a given constant representing the relative size of the manipulator with respect to the stroke. In the simulation, $\lambda = 2$.

Combining the objective and constraints together, the optimal design problem of a Gough-Stewart platform is formulated as follows.

Problem 3: Optimal design of a Gough-Stewart platform

Find a set of optimal design parameters α such that

$$\begin{aligned}
\max_{\alpha} \quad & l \\
\text{subject to} \quad & \kappa(J_z(X, \rho, \alpha)) \geq 0.2; \\
& \kappa(J_\Psi(X, \rho, \alpha)) \geq 0.2; \\
& \rho_0 - 0.5 \leq \rho_i(X, \alpha) \leq \rho_0 + 0.5; \\
& 0 \leq \text{Angle}(\mathbf{L}_j^w, \mathbf{L}_{j0}^w) \leq 55^\circ; \\
& 0 \leq \text{Angle}(\mathbf{L}_j^b, \mathbf{L}_{j0}^b) \leq 55^\circ; \\
& \text{dist}(\mathbf{L}_k, \mathbf{L}_l) \geq 0.04; \\
& \eta(X, \rho, \alpha) \geq 30^\circ; \\
& a + b + \rho_0 = 2; \\
& a, \ b, \ z_c \in [0, 2], \quad \rho_0 \in [0.5, 2], \\
& \vartheta, \ \varphi \in [0, \frac{\pi}{3}];
\end{aligned}$$

for all $X \in W$, $i, j, k, l = 1, \cdots, 6$ and $k < l$. ■

By applying the CRS algorithm, the optimal design parameters and the corresponding maximal side length are obtained, as shown in Table II. Fig. 10-(a) shows a scaled model of the resulting manipulator at its home configuration. The inclusion of link interference constraints leads to a more practical realization, while a sole maximization of effective regular workspace with no consideration on mechanical interference [31] results in a zero radius of the moving platform ($b \approx 0$) and coincidence of the close S-joints pairwisely ($\vartheta, \varphi \approx \pi/3$), both on the base and the moving platform. This implies that both the base and the moving platform degenerate to equilateral triangles.

Fig. 10-(b) shows workspace cross sections generated by the resulting manipulator at $z = z_c - l^*$, z_c, and $z_c + l^*$, respectively. The shadowed square, which is contained in all three cross sections, is the corresponding cross section of the maximal effective regular workspace. At cross section $z = z_c + l^*$, the maximal effective workspace touches the workspace boundary produced by the resulting manipulator.

a	b	ρ_0	ϑ	φ	z_c	$\Phi^* = l^*$
0.5860	0.2105	1.2035	1.0027	0.9397	1.0940	0.2596

TABLE II
OPTIMAL RESULTS FOR THE GOUGH-STEWART PLATFORM

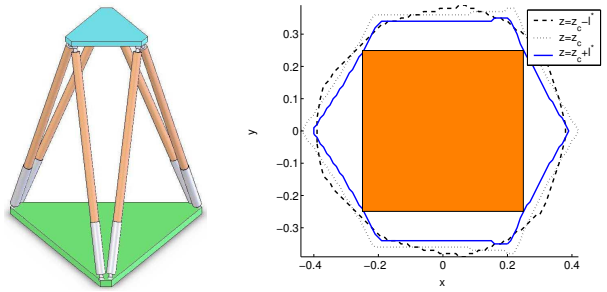

(a) (b)

Fig. 10. (a) A scaled model of the resulting Gough-Stewart platform; (b) workspace cross sections of the optimal manipulator.

Fig.11 shows distribution of the dexterity indices $\kappa(J_z)$ and $\kappa(J_\Psi)$ at cross section $z = z_c$ of the resulting maximal effective regular workspace with zero tilting angle. Fig. 12 shows a worst case for $\kappa(J_z)$, where the minimal κ is very close to the prescribed threshold 0.2. This indicates that the dexterity constraint (12) becomes active.

C. Discussion and Comparison

Usually people solve the optimal design problem 1 by exhaustive search as follows [7][11][4].

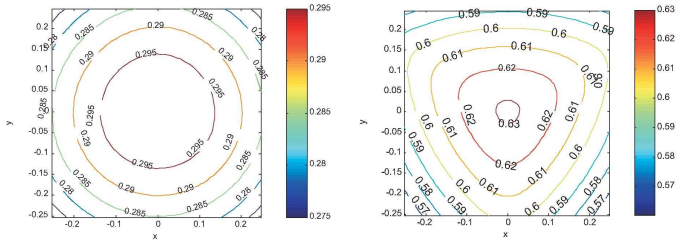

(a) (b)

Fig. 11. Contour plots of (a) $\kappa(J_z)$ and (b) $\kappa(J_\Psi)$ at $z = z_c$ and $\eta = 0$.

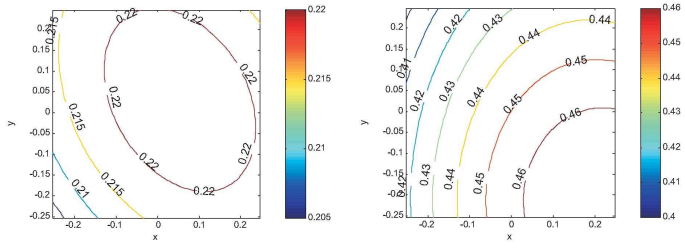

(a) (b)

Fig. 12. Contour plots of (a) $\kappa(J_z)$ and (b) $\kappa(J_\Psi)$ at $z = z_c + l^*$ and $\eta = -30^\circ$ about the direction $(-\frac{\sqrt{3}}{2}, \frac{1}{2}, 0)$.

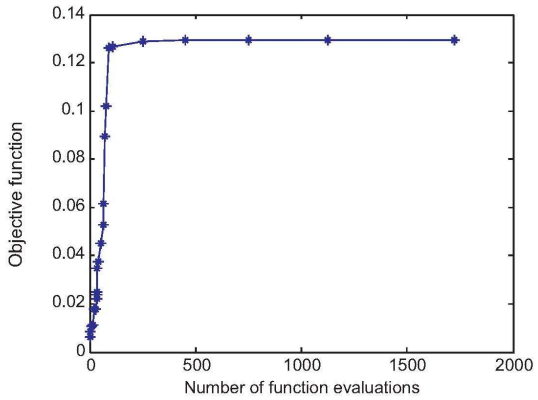

Fig. 13. A typical CRS convergence process for the optimal design problem of the Delta robot

- Discretize the design parameter space $P = \{P_1, \cdots, P_t\}$;
- For each $P_i, i = 1, \cdots, t$, discretize the regular workspace, check all constraints and compute the objective function;
- Find the largest objective and the corresponding best value for design parameters.

Clearly, this method involves discretization of both design parameter space and workspace. The search accuracy highly depends on fineness of discretization. Once a fine discretization is applied, however, the search will be very slow. Our proposed technique need only to discretize workspace. It searches the optimum in the continuous design parameter space. Also the CRS technique features a fast convergence rate when search points are not in the vicinity of the optimum. Therefore, the proposed technique is expected to improve the convergence rate greatly. Let's investigate the convergence of the two methods when they're applied to solve Problem 2, optimal design of a Delta robot. The design parameter space $P = \{(a, b, z_c)|a, b \in [0, 1], z_c \in [-1, 0]\}$ is discretized by step 0.01. By using a notebook computer with an Intel Pentium(M) processor of 1.3G Hz and the Matlab environment, the exhaustive search took 3.1776e+003 seconds to attain the optimum 0.1287 with optimal parameters (0.58, 0.41, -0.69). In contrast, the CRS algorithm took only 138.3290 seconds, 4.35% of running time of the exhaustive search, to reach the real optimum 0.1296.

A typical CRS convergence process for optimization of the rotational Delta robot is shown in Fig. 13. The CRS algorithm converged after 23 iterations (improvements). It is noted that the algorithm converges extremely fast initially. It takes only 253 function evaluations, which is less than 15% of the total effort, to approach the objective of 0.12872, which is about 99.3% of the optimum. The optimization process, however, becomes slow in a close neighborhood of the optimum.

V. Conclusion

In this paper, we presented a systematic procedure for optimal design of parallel manipulators. A unified and practical formulation for maximization of effective regular workspace was proposed. By investigating the nature of the optimal design problem, a direct search method, the CRS technique, was introduced to solve the problem. Optimal design of a rotational Delta robot and a Gough-Stewart platform were carried out and the results show the effectiveness of the design procedure. The CRS algorithm was proved efficient and reliable and can be a good alternative to solve optimal design problems of parallel manipulators.

Acknowledgment

The authors would like to thank the editors and unnamed reviewers for their valuable comments.

References

[1] J-P. Merlet. Designing a parallel manipulator for a specific workspace. *The International Journal of Robotics Research*, 16(4):545–556, 1997.

[2] J.-P. Merlet. An improved design algorithm based on interval analysis for spatial parallel manipulator with specified workspace. In *Proceedings of IEEE International Conference on Robotics and Automation*, pages 1289–1294, 2001.

[3] E. Ottaviano and M. Ceccarelli. Optimal design of CAPAMAN (Cassino parallel manipulator) with a specific orientation workspace. *Robotica*, 20(2):159–166, 2002.

[4] A. Kosinka, M. Galicki, and K. Kedzior. Designing and optimization of parameters of delta-4 parallel manipulator for a given workspace. *Journal of Robotic Systems*, 20(9):539–548, 2003.

[5] Y.J. Lou, G.F. Liu, J.J. Xu, and Z.X. Li. A general approach for optimal kinematic design of parallel manipulators. In *Proceedings of IEEE International Conference on Robotics and Automation*, pages 3659 – 3664, 2004.

[6] M. Guillot C.M. Gosselin. The synthesis of manipulators with prescribed workspace. *Transactions of the ASME, Journal of Mechanical Design*, 113(3):451–455, 1991.

[7] R.E. Stamper, L.W. Tsai, and G.C. Walsh. Optimization of a three dof translational platform for well-conditioned workspace. In *Proceedings of IEEE International Conference on Robotics and Automation*, pages 3250–3255, 1997.

[8] C. Gosselin and J. Angeles. The optimum kinematic design of a planar three-degree-of-freedom parallel manipulator. *ASME Journal of mechanisms, Transmissions, and Automation in Design*, 110, 1988.

[9] C. Gosselin and J. Angeles. The optimum kinematic design of a spherical three-dof-of-freedom parallel manipulator. *ASME Journal of mechanisms, Transmissions, and Automation in Design*, 111, 1989.

[10] H. H. Pham and I-M. Chen. Optimal synthesis for workspace and manipulability of parallel flexure mechanism. In *Proceeding of the 11th World Congress in Mechanism and Machine Science, Apr. 1-4, 2004,2004,edited by Tian Huang*, 2004.

[11] Michael Stock and Karol Miller. Optimal kinematic design of spatial parallel manipulators: Application of linear delta robot. *Transactions of the ASME, Journal of Mechanical Design*, 125(2):292–301, 2003.

[12] D. Chablat, P. Wenger, F. Majou, and J.-P. Merlet. An interval analysis based study for the design and the comparison of three-degrees-of-freedom parallel kinematic machines. *The International Journal of Robotics Research*, 23(6):615–624, 2004.

[13] D. Chablat and P. Wenger. Architecture optimization of a 3-dof translational parallel mechanism for machining applications, the orthoglide. *IEEE Transactions on Robotics and Automation*, 19(3):403–410, 2003.

[14] Y.J. Lou, D.J. Zhang, and Z.X. Li. Optimal design of a parallel machine based on multiple criteria. In *Proceedings of IEEE International Conference on Robotics and Automation*, 2005.

[15] Y.X. Su, B.Y. Duan, and C.H. Zheng. Genetic design of kinematically optimal fine tuning stewart platform for large spherical radio telescope. *Mechatronics*, 11:821–835, 2001.

[16] M. Arsenault and R. Boudreau. The synthesis of three-degree-of-freedom planar parallel mechanisms with revolute joints (3-RRR) for an optimal singularity-free workspace. *Journal of Robotic Sytems*, 21(5):259–274, 2004.

[17] F. Hao and J.-P. Merlet. Multi-criteria optimal design of parallel manipulators based on interval analysis. *Mechanism and Machine Theory*, 40(1):157–174, 2005.

[18] R.L. Anderson. Recent advances in finding best operating conditions. *Journal of the American Statistical Association*, 48(264):789–798, 1953.

[19] S.H. Brooks. A discussion of random methods for seeking maxima. *Operations research*, 6(2):244–251, 1958.

[20] L.A. Rastrigin. The convergence of the random search method in the extremal control of a many-parameter system. *Automation and Remote Control*, 24:1337–1342, 1963.

[21] Dean C. Karnopp. Random search techniques for optimization problems. *Automatica*, 1(1):111–121, 1963.

[22] M.W. Heuckroth, J.L. Gaddy, and L.D. Gaines. An examination of the adaptive random search technique. *AIChE Journal*, 22(4):744–750, 1976.

[23] L. W. Tsai. Kinematics of a three-dof platform with three extensible limbs. *Recent Advances in Robot Kinematics: Analysis and Control, J. Lenaric and V. Parenti-Castelli, Eds. Norwell, MA: Kluwer*, pages 49–58, 1996.

[24] R. Clavel. Delta, a fast robot with parallel geometry. In *Proc. 18th International Symposium on Industrial Robots*, pages 91–100, 1988.

[25] H. Lipkin and J. Duffy. Hybrid twist and wrench control for a robotic manipulator. *Transactions of ASME, Journal of Mechanisms, Transmissions, and Automation in Design*, 110(2):138–144, 1988.

[26] A. Törn and A. Žilinskas. *Global Optimization*. Springer-Verlad, 1st edition, 1989.

[27] R. Goulcher and J.J. Casares Long. The solution of steady-state chemical engineering optimisation problems using a random search algorithm. *Computers and Chemical Engineering*, 2(1):33–36, 1978.

[28] J.R. Banga and W.D. Seider. Global optimization of chemical processes using stochastic algorithms. *State of the Art in Global Optimization: Computational Methods and Applications, C.A. Floudas and P. M. Pardalos (Eds.), Kluwer Academic Publishers*, pages 563–583, 1996.

[29] Francisco J. Solis and Roger J-B. Wets. Minimization by random search techniques. *Mathematics of operations research*, 6(1):19–30, 1981.

[30] F. Sternheim. Tridimensional computer simulation of a parallel robot. Results for the 'DELTA4' Machine. In *Proc. 18th International Symposium on Industrial Robots*, pages 333–340, 1988.

[31] Y.J. Lou, G.F. Liu, N. Chen, and Z.X. Li. Optimal design of parallel manipulators for maximum effective regular workspace. In *Proceedings of IEEE/RSJ International Conference on Intelligent Robots and Systems*, pages 1208–1213, 2005.